

On Redistributed Energy Fluxes in Topographic Scattering Problems

Peter Müller

Department of Oceanography, School of Ocean and Earth Science and Technology,
University of Hawaii, Honolulu

Abstract. The scattering of infinitesimal inviscid internal waves at topography redistributes the incoming energy flux in wave number and physical space. This energy flux redistribution describes the scattering process most succinctly. The definitions of the redistributed energy flux in wave number space and in various subspaces are given. All of the incident energy flux is redistributed in wave number space. The total redistributed energy flux in subspaces is only a fraction of the total incident flux and depends on the choice of subspace. These concepts are illustrated with examples from the scattering at an infinite straight slope, random infinitesimal topography, and finite topography in a finite-depth ocean.

1. Introduction

The energy flux, as opposed to the energy or shear, is the most fundamental quantity in analyzing the scattering of infinitesimal inviscid internal waves at topography. This is because the conservation of energy implies that the total energy flux incident onto the topography equals the total energy flux scattered away from the topography. The incoming energy flux is only redistributed both in physical and wave number space. The details of this redistribution depend on the frequency and wave number of the incident wave and on the topography. The definition and interpretation of the redistributed energy flux is straightforward in the complete space of independent variables that describe the scattering process. In this space all of the incident flux is redistributed. In applications one usually considers the redistribution in some reduced space. The redistributed energy flux in such reduced spaces is smaller than the incident energy flux and depends on the choice of the reduced space. We illustrate these concepts by examples taken from the scattering at random infinitesimal topography, the reflection at an infinite straight slope, and the scattering at finite topography in a finite depth ocean. The incident internal wave field in all these examples is assumed to be a typical deep ocean internal wave field described by the Garrett and Munk spectrum.

2. The Redistributed Energy Flux

The energy flux vector is given by

$$\mathbf{F} = \mathbf{v} E \quad (2.1)$$

where \mathbf{v} is the group velocity vector and E the energy. The flux normal to a surface with normal vector \mathbf{n} is

$$\mathbf{F} \cdot \mathbf{n} = \mathbf{v} \cdot \mathbf{n} E \quad (2.2)$$

Let the slope or vertical inclination of the surface be $\gamma = \tan \varphi_0$. One can then orient the horizontal coordinates such that $0 \leq \varphi_0 \leq \pi/2$ and $\mathbf{n} = (1 + \gamma)^{\frac{1}{2}} (-\gamma, 0, 1)$. The normal vector is assumed to point out of the surface into the fluid. A plane internal wave is characterized by its wave number vector $\mathbf{k} = (k_1, k_2, k_3)$. The frequency ω is given by the dispersion relation. Scattering at topography does not change the frequency. It is therefore advantageous to work in a representation that includes the frequency. Here we choose the frequency ω , the magnitude $\alpha = (k_1^2 + k_2^2)^{\frac{1}{2}}$ of the horizontal wave number vector, the azimuthal direction $\phi = \arctan(k_2/k_1)$, and the sign $s = \text{sgn}(k_3)$ of the vertical wave number component as the independent variables to describe a plane internal wave. Then

$$\mathbf{v} \cdot \mathbf{n} = -\frac{1}{(1 + \gamma^2)^{\frac{1}{2}}} \frac{1}{\alpha} \left(\frac{\omega^2 - f^2}{N^2 - f^2} \right) \left(\frac{N^2 - \omega^2}{\omega^2} \right)^{\frac{1}{2}} \left[\gamma(N^2 - \omega^2) \cos \phi + s(\omega^2 - f^2)^{\frac{1}{2}} \right] \quad (2.3)$$

where f is the Coriolis frequency and N the Brunt-Väisälä frequency. Expressions for other independent variables can be obtained by standard transformations. Figure 1 shows the areas in (ω, ϕ, s) -space for which $\mathbf{v} \cdot \mathbf{n} \geq 0$.

The flux incident on a surface with normal vector \mathbf{n} is

$$F_i(\omega, \alpha, \phi, s) = \begin{cases} |\mathbf{v} \cdot \mathbf{n}| E_i(\omega, \alpha, \phi, s), & \text{if } \mathbf{v} \cdot \mathbf{n} \leq 0 \\ 0, & \text{if } \mathbf{v} \cdot \mathbf{n} \geq 0 \end{cases} \quad (2.4)$$

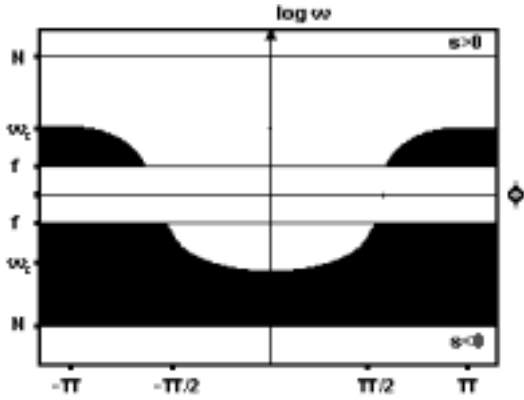


Figure 1. Areas (shaded) in (ω, ϕ, s) -space for which $\mathbf{v} \cdot \mathbf{n} \geq 0$.

The scattered energy flux is

$$F_s(\omega, \alpha, \phi, s) = \begin{cases} |\mathbf{v} \cdot \mathbf{n}| E_s(\omega, \alpha, \phi, s), & \text{if } \mathbf{v} \cdot \mathbf{n} \geq 0 \\ 0, & \text{if } \mathbf{v} \cdot \mathbf{n} \leq 0 \end{cases} \quad (2.5)$$

Here E_i and E_s are the energy spectra of the incident and scattered wave field. Note that F_i and F_s are both defined to be positive. In scattering problems the incident energy spectrum is specified. The scattered energy spectrum is calculated from some scattering theory. In applications the incident energy spectrum is often specified to be

$$\begin{aligned} E_i(\omega, \alpha, \phi, s) &= E_{GM}(\omega, \alpha, \phi, s) \\ &= \frac{1}{2\pi} \frac{1}{2} E_{GM}(\omega, \alpha) \end{aligned}$$

where

$$E_{GM}(\omega, \alpha) = E_0 b^2 N_0 N B(\omega) \frac{A(\frac{\alpha}{\alpha_*})}{\alpha_*} \quad (2.6)$$

is the horizontally isotropic and vertically symmetric Garrett and Munk spectrum (henceforth GM-spectrum, *Munk* 1981), given here in standard notation.

The basic diagnostic tool to describe the effect of scattering is the redistributed energy flux

$$D(\omega, \alpha, \phi, s) = F_s(\omega, \alpha, \phi, s) - F_i(\omega, \alpha, \phi, s) \quad (2.7)$$

Since the incident and scattered $(\omega, \alpha, \phi, s)$ -values are mutually exclusive, a given set of values is either an incoming or a scattered wave. All of the incident flux is redistributed in $(\omega, \alpha, \phi, s)$ -space. The total redistributed energy flux in $(\omega, \alpha, \phi, s)$ -space is defined as the integral over the positive (or negative) lobe of $D(\omega, \alpha, \phi, s)$, i.e., by

$$T = \frac{1}{2} \int d\omega \int d\alpha \int d\phi \sum_s \int |D(\omega, \alpha, \phi, s)| \quad (2.8)$$

and the above statement becomes

$$T = \int d\omega \int d\alpha \int d\phi \sum_s F_i(\omega, \alpha, \phi, s) =: F_i \quad (2.9)$$

One can also determine the redistributed fluxes and the total redistributed fluxes in various reduced spaces such as

$$D(\omega, \alpha) = \int d\phi \sum_s D(\omega, \alpha, \phi, s) \quad (2.10)$$

$$T_1 = \frac{1}{2} \int d\omega \int d\alpha |D(\omega, \alpha)| \quad (2.11)$$

or

$$D(\alpha) = \int d\omega D(\omega, \alpha) \quad (2.12)$$

$$T_2 = \frac{1}{2} \int d\alpha |D(\alpha)| \quad (2.13)$$

For scattering at topography, there is no redistribution in frequency space

$$D(\omega) = \int d\alpha D(\omega, \alpha) \equiv 0 \quad (2.14)$$

Instead one introduces

$$D^+(\omega) = \frac{1}{2} \int d\alpha |D(\omega, \alpha)| \quad (2.15)$$

which describes the frequencies where most of the redistribution occurs.

In the following we illustrate these concepts with a few examples.

3. Reflection at a Flat Bottom

Reflection at a flat bottom $z = 0$ is the most trivial reflection problem. Internal wave kinematics implies that a downward propagating wave ($\omega, \alpha, \phi, s = +1$) is reflected into an upward propagating wave ($\omega, \alpha, \phi, s = -1$). Thus

$$F_s(\omega, \alpha, \phi, s) = F_i(\omega, \alpha, \phi, -s) \quad (3.1)$$

and

$$D(\omega, \alpha, \phi, s) = \begin{cases} -F_i(\omega, \alpha, \phi, s), & \text{if } s = +1 \\ F_i(\omega, \alpha, \phi, -s), & \text{if } s = -1 \end{cases} \quad (3.2)$$

The flux is redistributed from downward propagating waves ($s = +1$) to upward propagating waves ($s = -1$). There is no redistribution in (ω, α, ϕ) -space

$$D(\omega, \alpha, \phi) = \sum_s D(\omega, \alpha, \phi, s) \equiv 0 \quad (3.3)$$

The total redistributed energy flux in $(\omega, \alpha, \phi, s)$ -space equals the total downward energy flux

$$T = \int d\omega \int d\alpha \int d\phi F_i(\omega, \alpha, \phi, s = +1) =: F_3 \quad (3.4)$$

For the GM-spectrum (2.6) one finds $F_3 = 17.6 \text{ mW m}^{-2}$, if $N = 0.4 \text{ cph}$ (deep ocean), and $f = 0.042 \text{ cph}$ (mid latitudes).

4. Scattering at Random Infinitesimal Topography

The scattering at random infinitesimal topography has been studied by perturbation methods by various authors (e.g., *Cox and Sandstrom, 1962; Rubenstein, 1988; Müller and Xu, 1992*). Here we draw on the results of *Müller and Xu*.

Consider random infinitesimal topography

$$z = h(x, y) \quad (4.1)$$

where $h(x, y)$ is a statistically homogeneous random field with zero mean and spectrum $H(\alpha)$. An incident wave with wave number α that interacts with

bottom component α' is scattered to wave number $\alpha'' = \alpha + \alpha'$ (Bragg scattering). The incident flux is downward. The scattered flux is upward. The total redistributed flux in $(\omega, \alpha, \phi, s)$ -space is thus F_3 which is 17.6 mW m^{-2} for the GM-spectrum.

Figure 4 shows the redistributed energy flux $D(\omega, \alpha)$ in (ω, α) -space. The energy flux is redistributed from low to high wave numbers, most efficiently at low frequencies. The total redistributed energy flux in (ω, α) -space is 1.2 mW m^{-2} , only about 6.8% of the total incoming flux of 17.6 mW m^{-2} .

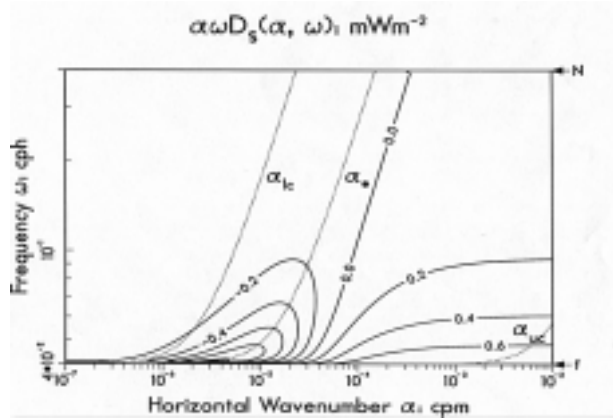


Figure 2. {

Contours of redistributed energy flux $D(\alpha, \omega)$ horizontal wave number and frequency in a variance-conserving representation. The dotted lines are the low wave number cutoff $\alpha_{lc}(\omega)$, the bandwidth $\alpha(\omega)$ and high wave number cutoff $\alpha_{uc}(\omega)$ of the Garrett and Munk spectrum. (From *Müller and Xu, 1992*).

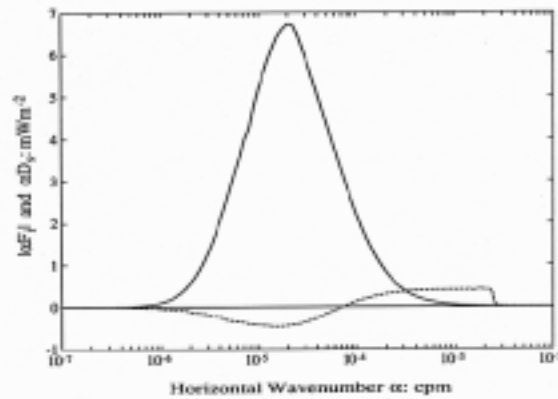


Figure 3. Incident energy flux $F_i(\alpha)$ (solid line) and redistributed energy flux $D(\alpha)$ (dashed line) as a function of horizontal wave number in a variance-conserving representation. (From *Müller and Xu, 1992*).

Figure 3 shows the incident energy flux $F_i(\alpha)$ and the redistributed energy flux $D(\alpha)$. $D(\alpha)$ again exhibits the transfer from low to high wave numbers seen in Figure 4. However, the total redistributed energy flux in α -space is 1.14 mW m^{-2} , slightly less than the total redistributed energy flux in (ω, α) -space. During frequency integration of $D(\omega, \alpha)$ some cancellations of positive and negative contributions occur. The zero line of $D(\omega, \alpha)$ depends on frequency and wave number (see Figure 4). The cancellations are, however, small. Figure 4 displays the incident energy flux $F_i(\omega)$ and $D^+(\omega)$ and again shows that most of the redistribution energy occurs at low frequencies.

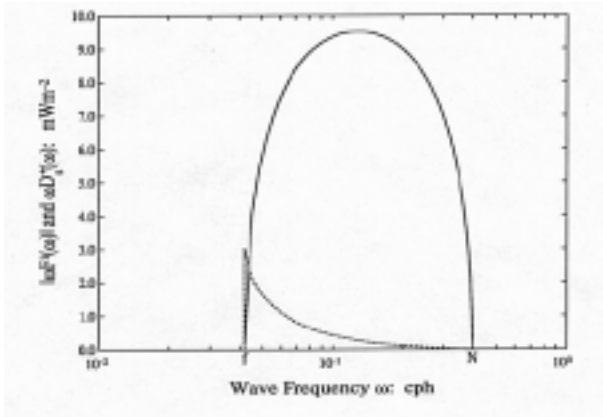


Figure 4. Incident energy flux $F_i(\omega)$ (solid line) and energy flux $D^+(\omega)$ (dashed line) as a function of frequency in a variance-conserving representation. (From Müller and Xu, 1992.)

5. Reflection at an Infinite Straight Slope

The reflection of an incident GM-spectrum off an infinite straight slope was first calculated by *Eriksen* (1985). Here we use results given in *Müller and Xu* (1992).

The reflection laws are algebraically quite complex. The case of normal incidence is considered in Figure 5. Both the incident and reflected wave number lie in the (k_1, k_3) -plane. Figure 5 shows the regions of permissible incident waves and the regions to which these incident waves are reflected. A particular role in this diagram is played by the frequency cone that has an inclination $\theta = \arctan(k_3/k_1)$ perpendicular to the bottom slope. This is the cone of critical frequency

$$\omega_c^2 = N^2 \sin^2 \varphi_0 + f^2 \cos^2 \varphi_0 \quad (5.1)$$

Incident waves of critical frequency are reflected to waves with infinite wave number and zero group velocity. The incident energy flux cannot propagate away from the boundary. The energy increases without bound. The behavior of the reflection process is different for sub- and supercritical frequencies. The areas of sub- and supercritical frequencies are also indicated in Figure 5.

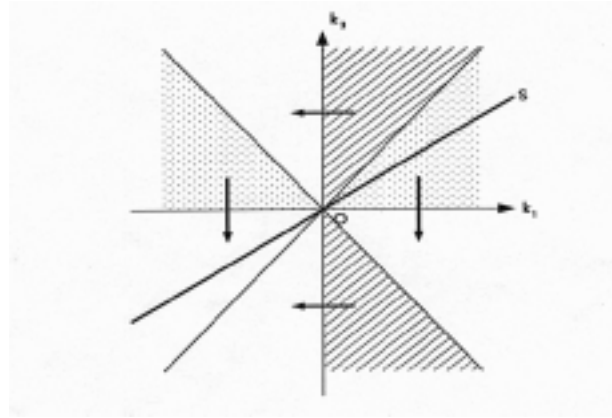


Figure 5. Regions of permissible incident and reflected waves in the horizontal-vertical wave number plane. The heavy solid straight line represents the bottom slope. The light solid lines represent the critical frequency cone. The cross-hatched and stippled regions are permissible incident wave numbers. For the cross-hatched regions the reflection is subcritical, for the stippled region the reflection is supercritical. The regions to which the incident wave numbers become reflected are indicated by the arrows. (From Müller and Xu, 1992.)

The incident and redistributed energy fluxes $F_i(\omega, \alpha)$ and $D(\omega, \alpha)$ are shown in Figure 6 as a function of horizontal wave number for three different frequencies. There is a redistribution from medium to low and high wave numbers. The total incident energy flux is the flux normal to the slope. It is 18.2 mW m^{-2} for the GM-spectrum and thus slightly larger than the total vertical energy flux of 17.6 mW m^{-2} considered in the previous section. The total redistributed energy flux in (ω, α) -space is 3.89 mW m^{-2} or about 21% of the incoming flux.

The fluxes $F_i(\alpha)$ and $D(\alpha)$ in wave number space are shown in Figure 7. The flux is mainly redistributed from medium to high wave numbers, with only a small fraction reflected to low wave numbers. The total redistributed flux in wave number space is 2.90 mW m^{-2} or about 16% of the total incoming flux. Most of the redistribution occurs at frequencies around the critical frequency as can be seen in Figure 8 which shows $F_i(\omega)$ and $D^+(\omega)$. Note that

$F_i(\omega)$ shows a characteristic dip at $\omega = \omega_c$ which is absent from the frequency spectrum of the vertical flux shown in Figure 4. The incident wave number spectra $F_i(\alpha)$ on the other hand look very similar for the vertical and normal-to-slope flux (Figure 3 and Figure 7).

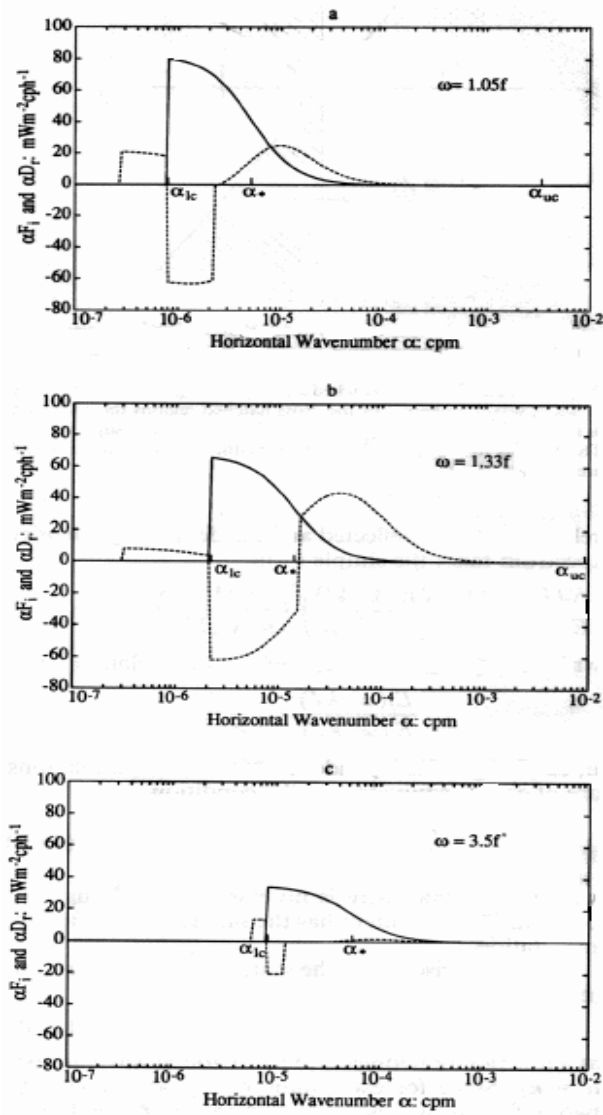


Figure 6. Reflection at a straight slope. Incident energy flux $F_i(\alpha, \omega)$ (solid line) and redistributed energy flux $D(\alpha, \omega)$ (dashed line) as a function of horizontal wave number for three different frequencies in a variance-conserving representation. The bottom slope is $\gamma = 0.07$ and the critical frequency is $\omega_c = 1.2f$. The wave numbers α_{lc} , α_* and α_{uc} are the low wave number cutoff, bandwidth, and high wavenumber cutoff of the Garrett and Munk spectrum. (From Müller and Xu, 1992).

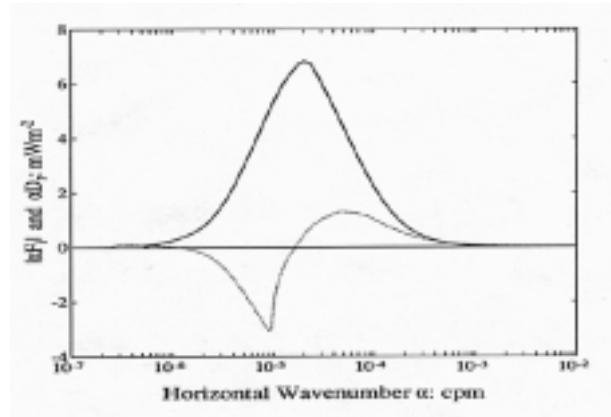


Figure 7. Reflection at a straight slope. Incident energy flux $F_i(\alpha)$ (solid line) and redistributed energy flux $D(\alpha)$ (dotted line) as a function of horizontal wave number in a variance-conserving representation. (From Müller and Xu, 1992).

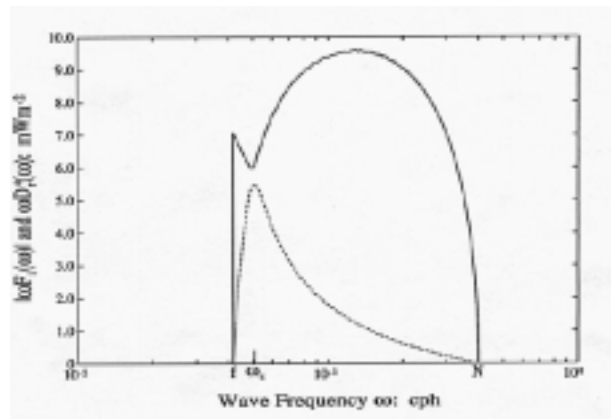


Figure 8. Reflection at a straight slope. Incident energy flux $F_i(\omega)$ (solid line) and energy flux $D^+(\omega)$ (dashed line) as a function of frequency in a variance-conserving plot. The bottom slope is $\gamma = 0.07$ and the critical frequency is $\omega_c = 1.2f$. (From Müller and Xu, 1992).

6. Scattering at Finite Topography

The scattering at finite topography in a finite depth ocean is considered in two papers by Müller and Liu (1999 a, b). The wave field is incident from the side onto either a slope shelf configuration or a ridge configuration (Figure 9). The study is restricted to the two-dimensional case of normal incidence. Modes are used. For the slope shelf configuration the incident wave field comes from the deep ocean side. For the ridge configuration one can consider the incident wave field coming from just one

side or the symmetric situation that the wave field is incident from both sides.

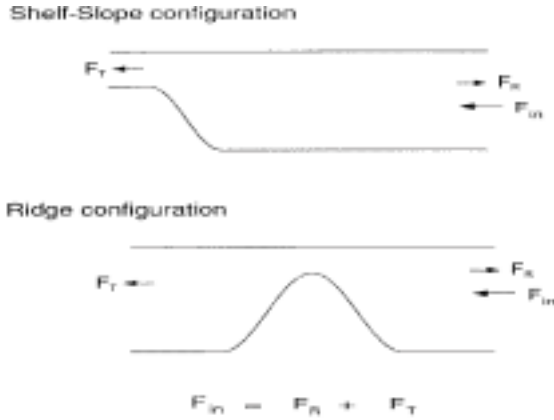


Figure 9. Configurations for the scattering at finite topography.

For the scattering problem one has to distinguish between the waves transmitted (or forward scattered) onto the shelf (or across the ridge) and the waves reflected (or back scattered) to the deep ocean. The energy flux is not only redistributed in wave number but also in physical space. As a complete set of independent variables one may thus use (ω, n, μ, x) where ω is the frequency as before, n the mode number, $\mu = \text{sgn}(k_1)$ the horizontal direction, and $x = \pm \infty$ the location in physical space. Assume that the incident field comes from the right hand side. Then the incident field is characterized by $\mu = -1$ and $x = +\infty$, the transmitted field by $\mu = -1$ and $x = -\infty$, and the reflected field by $\mu = +1$ and $x = +\infty$.

The two-dimensional problem only considers normal incidence. The along-topography wave number k_2 is zero. To complete the problem one also needs to calculate the scattering for oblique incidence. However, a consistent physical problem can be obtained by considering the total energy flux onto the topography, integrated over all azimuthal directions.

$$F(\omega, n) = \int_{-\pi/2}^{\pi/2} d\phi E(\omega, \alpha, \phi) v_h(\omega, n) \cos \phi \quad (6.1)$$

Here v_h is the magnitude of the horizontal group velocity vector. Note that F is a horizontal flux. Assume this integrated flux to be the incident flux in the two-dimensional problem.

$$F_i(\omega, n) = F(\omega, n, \mu = -1, x = +\infty) = F(\omega, n) \quad (6.2)$$

We thus assume that all incident waves are scattered as if they had normal incidence. If we substitute the horizontally isotropic GM-spectrum into (6.1) we find

$$F_i(\omega, n) = \frac{1}{\pi} E_{GM}(\omega, n) v_h(\omega, n) \quad (6.3)$$

This incident flux spectrum together with the reflected flux spectrum

$$F_r(\omega, n) = F(\omega, n, \mu = +1, x = +\infty) \quad (6.4)$$

and the transmitted flux spectrum

$$F_t(\omega, n) = F(\omega, n, \mu = -1, x = -\infty) \quad (6.5)$$

is shown in Figure 10 for the scattering at a half cosine slope.

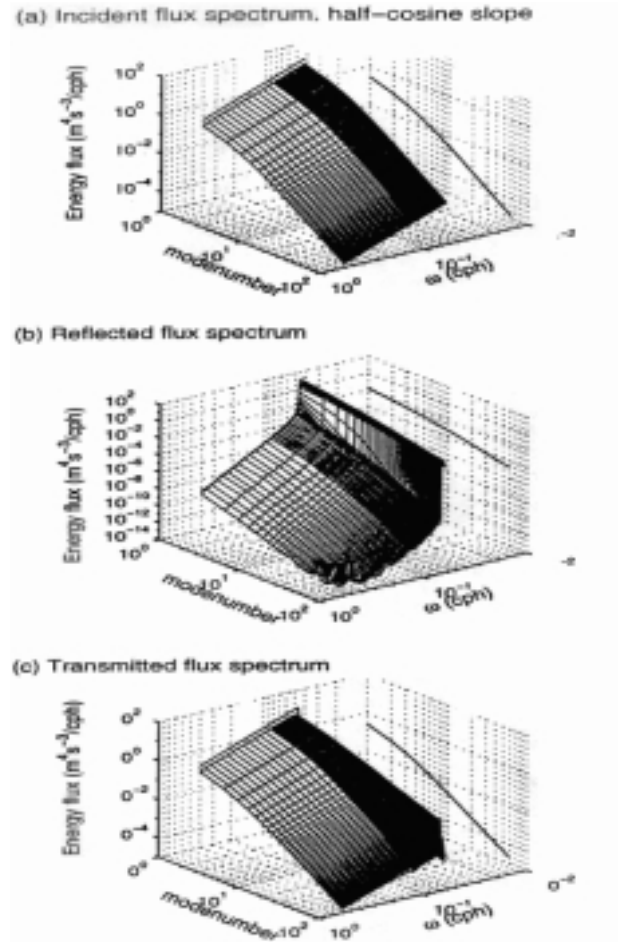


Figure 10. Incident, reflected, and transmitted flux spectrum for a half-cosine slope. (From Müller and Liu, 1999b.)

The total incident flux is 560 W m^{-1} when vertically integrated over the water column. This corresponds to a local flux of the order of 100 mW m^{-2} for a 5 km deep ocean. This horizontal flux is considerably larger than the vertical energy flux of 17.6 mW m^{-2} . In Figure 10, 91.4% of the incident flux is transmitted onto the shelf and 8.6% is reflected back into the deep ocean.

Redistribution in various reduced spaces can now be considered. The redistribution

$$D(\omega, n, \mu) = \sum_{x=\pm\infty} D(\omega, n, \mu, x) = \begin{cases} F_t(\omega, n) - F_i(\omega, n), & \text{if } \mu = -1 \\ F_r(\omega, n), & \text{if } \mu = +1 \end{cases} \quad (6.6)$$

in (ω, n, μ) -space is shown in Figure 11. The redistribution is only significant for low and near critical frequencies. The major redistribution is from low mode number leftward propagating waves to low and medium mode number rightward propagating waves. There is also a transfer from low to medium mode number leftward propagating waves at near critical frequencies. The total redistributed energy flux is about 8.9% of the total incident flux.

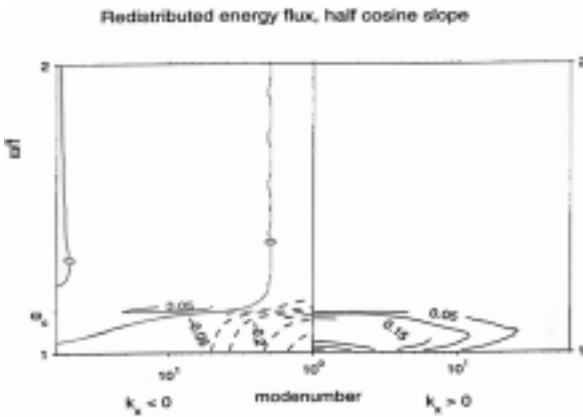


Figure 11. Redistributed energy flux $D(\omega, n, \mu)$ for the half cosine slope of figure 10. (From Müller and Liu, 1999b.)

The redistribution in (ω, n, μ) -space has to be distinguished from the redistributed energy flux

$$D(\omega, n, x) = \sum_{\mu} D(\omega, n, \mu, x) = \begin{cases} F_r(\omega, n) - F_i(\omega, n), & \text{if } x = +\infty \\ F_t(\omega, n), & \text{if } x = -\infty \end{cases} \quad (6.7)$$

in (ω, n, x) -space (not shown).

For a ridge configuration one can consider the symmetric case where a GM-spectrum is incident from both sides. Then

$$D(\omega, n, x) = F_y(\omega, n) + F_t(\omega, n) - F_i(\omega, n) \quad (6.8)$$

for both $x = \pm\infty$. This redistributed energy flux is shown in Figure 12. The redistribution is from low to medium mode numbers at low and near critical frequencies. Figure 13 shows the incident and redistributed energy fluxes $F_i(n, x)$ and $D(n, x)$. The energy flux is redistributed from the first and second mode to mode numbers around 10. The total redistributed energy flux is about 4.3% of the incident flux.

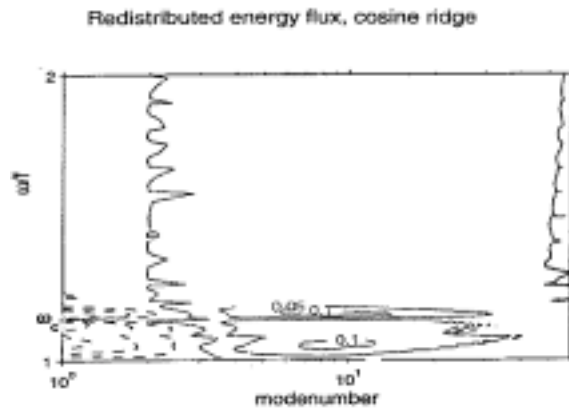


Figure 12. Redistributed energy flux $D(\omega, n, x)$ for a cosine ridge of depth ratio $\delta = 4/3$ and maximum slope $h_{max} = 0.01\pi$. (From Müller and Liu, 1999b.)

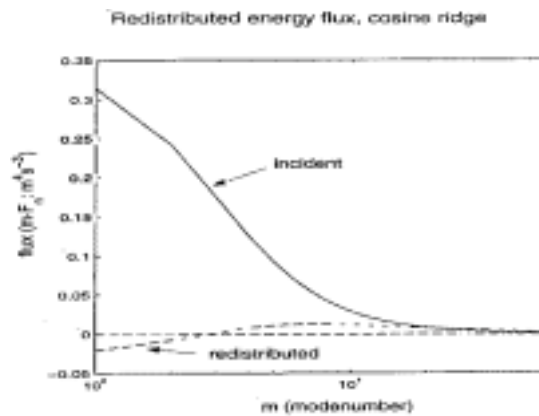


Figure 13. Incident energy flux $F_i(n, x)$ and redistributed energy flux $D(n, x)$ for the cosine ridge of figure 12. (From Müller and Liu, 1999b.)

7. Summary and Conclusions

The scattering of internal waves at topography is most succinctly described by the redistributed energy flux. Energy conservation implies that the total incoming energy flux equals the total outgoing flux. Since incoming and outgoing waves are characterized by different wave number vectors, the total redistribution in wave number space is equal to the total incident flux. Since scattering at topography does not change the frequency it is advantageous to use a representation that involves the frequency instead of the wave number vector. It is also helpful to atune the other components to the geometry of the problem. In some problems the location in physical space must also be considered. For various applications one considers the redistribution of the energy flux in reduced spaces. The total redistributed energy flux in these reduced spaces is only a fraction of the total incident flux and depends on the choice of the reduced space.

Scattering at topography is often implied in causing wave breaking and mixing. The redistributed energy flux is used to calculate the fraction of the incident energy flux that is scattered to high wave numbers beyond a critical wave number. This critical wave number is determined by the condition that the Richardson number of all waves up to that critical wave number is of the order of one. It is then argued that waves scattered to wave numbers higher than the critical wave number are likely to break and cause mixing. There are problems with these calculations. First, the critical wave number is not uniquely defined. Results depend on whether one works in vertical wave number, horizontal wave number or mode number space. Second, it is by no means clear that in a breaking wave field energy is extracted (and then converted to mixing and heat), only from high wave numbers larger than a critical wave number. Wave breaking is a process that is local in physical space and can be expected to be broad-banded in wave number space.

8. Acknowledgments

The author would like to thank Alexander Adams for his help in the preparation of this manuscript. This work was supported by the Office of Naval Research.

References

Cox, D. and H. Sandstrom, 1962: Coupling of internal and surface waves in water of variable depth.

J. Oceanogr. Soc. Japan (20th Anniversary Volume), 499-513.

Eriksen, C. C., 1982: Observation of internal wave reflection off sloping bottom. *J. Geophys. Res.*, 87, 525-538.

Müller, P. and Xu, N., 1992: Scattering of oceanic gravity waves off random bottom topography. *J. Phys. Oceanogr.*, Vol.22, No.5.

Müller, P. and Liu, X., 1999a: Scattering of internal waves at finite topography in two dimensions. Part 1: Theory and case studies. *J. Phys. Oceanogr.* (accepted for publication)

Müller, P. and Liu, X., 1999b: Scattering of internal waves at finite topography in two dimensions. Part 1: Spectral calculations and boundary mixing. *J. Phys. Oceanogr.* (accepted for publication)

Munk, W. H., 1981: Internal waves and small-scale processes. *Evolution of Physical Oceanography*, B. A. Warren and C. Wunsch, Eds., MIT Press, 264-291.

Rubenstein, D., 1988: Scattering of inertial waves by rough bathymetry. *J. Phys. Oceanogr.*, 18, 5-18